Chitosan scaffolds induce human dental pulp stem cells to neural differentiation: potential roles for spinal cord injury therapy

Jinlong Zhang[1] · Xiaohui Lu[2] · Guijuan Feng[2] · Zhifeng Gu[3] · Yuyu Sun[1] ·
Guofeng Bao[1] · Guanhua Xu[1] · Yuanzhou Lu[4] · Jiajia Chen[1] · Lingfeng Xu[2] ·
Xingmei Feng[2] · Zhiming Cui[1]

Abstract Cell-based transplantation strategies hold great potential for spinal cord injury (SCI) repair. Chitosan scaffolds have therapeutic benefits for spinal cord regeneration. Human dental pulp stem cells (DPSCs) are abundant available stem cells with low immunological incompatibility and can be considered for cell replacement therapy. The purpose of this study is to investigate the role of chitosan scaffolds in the neural differentiation of DPSCs in vitro and to assess the supportive effects of chitosan scaffolds in an animal model of SCI. DPSCs were incubated with chitosan scaffolds. Cell viability and the secretion of neurotrophic factors were analyzed. DPSCs incubated with chitosan scaffolds were treated with neural differentiation medium for 14 days and then neural genes and protein markers were analyzed by Western blot and reverse transcription plus the polymerase chain reaction. Our study revealed a higher cell viability and neural differentiation in the DPSC/chitosan-scaffold group. Compared with the control group, the levels of BDNF, GDNF, b-NGF, and NT-3 were significantly increased in the DPSC/chitosan-scaffold group. The Wnt/β-catenin signaling pathway played a key role in the neural differentiation of DPSCs combined with chitosan scaffolds. Transplantation of DPSCs together with chitosan scaffolds into an SCI rat model resulted in the marked recovery of hind limb locomotor functions. Thus, chitosan scaffolds were non-cytotoxic and provided a conducive and favorable microenvironment for the survival and neural differentiation of DPSCs. Transplantation of DPSCs might therefore be a suitable candidate for treating SCI and other neuronal degenerative diseases.

Jinlong Zhang, Xiaohui Lu, and Guijuan Feng contributed equally to this work.

✉ Xingmei Feng
  fengxingmeint@126.com

✉ Zhiming Cui
  cuizhiming2012@hotmail.com

[1] Department of Spine Surgery, The Second Affiliated Hospital of Nantong University, Nantong, Jiangsu Province 226001, People's Republic of China

[2] Department of Stomatology, Affiliated Hospital of Nantong University, Nantong, Jiangsu Province 226001, People's Republic of China

[3] Department of Rheumatology, Affiliated Hospital of Nantong University, Nantong, Jiangsu Province 226001, People's Republic of China

[4] Department of Cardiology Medical, Tongzhou First People's Hospital, Nantong, Jiangsu Province 226300, People's Republic of China

Introduction

Traumatic spinal cord injury (SCI) is one of the most devastating of all traumatic events in the world affecting the quality of life of young males and resulting in sensation disability and paralysis (Ceruti et al. 2009). The complicated pathophysiologic mechanisms underlying SCI include the loss of neurons and glial cells, axonal degeneration and destruction of the neural circuit (Zhang et al. 2013). Therefore, the development of a new strategy to restore the tissue structure and function of injured spinal cord remains a significant challenge. One of the promising approaches is cell transplantation therapy to replace the damaged or lost cells after SCI (Kim et al. 2011). Dental pulp stem cells (DPSCs) are a promising candidate for transplantation therapy, because DPSCs can be simply isolated from freshly extracted teeth; these cells can be highly proliferated, multilineage-differentiated and used as autologous transplants (Gronthos et al. 2000; Laino et al. 2005; d'Aquino et al. 2009; Giuliani et al. 2013). Moreover, their clinical utility is attributable to their simplicity and convenience of isolation, lack of ethical controversy and low immunogenicity (Huang et al. 2009). In recent years, DPSCs have been clearly shown to be useful for SCI treatment, based on convincing evidence that their administration results in functional recovery in various animal models (Sakai et al. 2012). DPSCs can differentiate into a variety of cell lineages, including odontoblasts, neural cells and glial cells (Gronthos et al. 2000; Laino et al. 2005; d'Aquino et al. 2009; Giuliani et al. 2013). DPSCs are more potent than bone marrow (BM) mesenchymal stem cells (MSCs) at promoting functional recovery after SCI (Sakai et al. 2012). In animal models, DPSCs transplanted into the brain differentiate into functional neurons or astrocytes in response to local environmental cues that appear to influence the fate of the surviving cells (Miura et al. 2003; Bray et al. 2014). Therefore, DPSCs represent a huge potential for the clinical application of cell replacement therapies for SCI.

Cells, scaffolds and growth factors are the three main factors for creating a tissue-engineered construct. The three-dimensional culture of exfoliated deciduous teeth stem cells (SHED) has become increasingly popular not only because of its influence on survival and differentiation but also because of the penetrative pores that facilitate in the growth of regenerating neural fibers from the host and grafted cells (Su et al. 2013). Dramatic and encouraging results of in vivo studies with bio-materials combined with stem cell transplantation have been reported in the treatment of SCI (Bozkurt et al. 2010). Chitosan is a cationic polymer derived from chitin and comprises β-(1–4)-glucosamine and N-acetyl-D-glucosamine monomeric units (Kas 1997). It has become an ideal material for diverse tissue engineering applications, as it is non-antigenic and non-toxic and promotes cell adhesion, proliferation and differentiation (Khor and Lim 2003; Wei et al. 2010). Previous data have shown the utility of chitosan scaffolds in promoting the differentiation of MSCs into neural cells that can then be used to treat traumatic brain injury (Shi et al. 2012). Our previous studies have demonstrated that chitosan scaffolds provide a conductive and favorable microenvironment for the neural differentiation of DPSCs. However, the mechanism remains unclear. In recent years, studies have shown that Wnt signals, primarily wnt3a, wnt5a and β-catenin, regulate the neural differentiation of rat adipose-derived stem cells (ADSCs; Yang et al. 2014). Wnt/β-catenin signaling is activated by the binding of Wnt ligands to the frizzled family of receptors. In the absence of Wnt ligands, β-catenin is phosphorylated by glycogen synthase kinase-3β (GSK-3β) and then degraded by the ubiquitin-proteasome system (Feng et al. 2013). When Wnt ligands bind to frizzled receptors, GSK-3β activity is inhibited and unphosphorylated β-catenin accumulates in the cytoplasm and translocates into the nucleus, where it promotes the transcription of a variety of the target gene (such as c-myc; Clevers 2006). We hypothesized that the implantation of chitosan scaffolds seeded with DPSCs after SCI wil permit the long-term survival of the transplanted cells.

The aim of the present study was to determine the neural differentiation and the associated mechanism of DPSCs on chitosan scaffolds for future tissue applications. As a first step, we examined the viability and secretion of neurotrophic factors of DPSC/chitosan scaffolds. Subsequently, we evaluated the neural differentiation of DPSCs and the role of Wnt/β-catenin signaling in this process. Finally, the results of our study will provide a foundation for the clinical application of DPSC/chitosan scaffold combinations as cell replacement therapies for SCI.

Materials and methods

Cell cultures

Normal human impacted third molars were collected from patients of 13–23 years of age ($n = 9$) after they had given informed consent, as approved by the Ethics Committee of the Affiliated Hospital of Nantong University. All subjects were free of carious lesions and oral infection. We isolated DPSCs by cleaning the tooth surface, cutting around the cemento-enamel junction by using sterilized dental fissure burs and then opening the tooth to reveal the pulp chamber. The pulp was then digested in a solution of 3 mg/ml collagenase type I for 1 h at 37 °C. Single-cell suspensions were

obtained by passing the digested tissues through a 70-μm cell strainer (BD Falcon). Cell suspensions of dental pulp were seeded into 25-cm^2 culture dishes and cultured in Dulbecco modified Eagle medium (DMEM) supplemented with 10 % fetal bovine serum (FBS), 100 U/ml penicillin and 100 μg/ml streptomycin at 37 °C under 5 % CO_2. The medium was changed every 3 days. Approximately 7–10 days after seeding, the cells became nearly confluent. Cells were passaged at the ratio of 1:3 when they reached 85 % to 90 % confluence. The adherent cells were released from the dishes with 0.25 % trypsin (Gibco, USA) and seeded into new fresh culture flasks. DPSCs were selected by fluorescence-activated cell sorting analysis. Briefly, cells were detached by using 0.02 % EDTA in phosphate-buffered saline (PBS) and pelleted (10 min at 1,000 rpm), washed in 0.1 % bovine serum albumin (BSA) in 0.1 M PBS at 4 °C and incubated in a solution of 1 ml antibody/9 ml 0.1 % BSA in 0.1 M PBS. Cells were washed in the same solution once and were processed for sorting. The mouse anti-human antibodies CD34, c-Kit and STRO-1 were from Santa Cruz. The cell populations were characterized by positive staining with anti-CD34, STRO-1 and c-Kit and the absence of CD45. DPSCs were further identified by osteogenic, chondrogenic and adipogenic differentiation (Feng et al. 2014a). For the growth of DPSCs on the chitosan scaffolds, DPSC were collected in culture medium when the cell confluence reached ≥ 90 %. Approximately 1×10^6 cells were added to each chitosan scaffold. According to the specific requirements of the experiment, the scaffolds were supplemented either with complete nutrient solution or neural differentiation medium.

Fabrication of chitosan porous scaffolds

Chitosan (0.2 g; 92.3 % deacetylated, average molecular weight = 2.2×10^4; Sigma, Aldrich) was dissolved in 10 ml acetic acid (1 %) to obtain a yellow-colored viscous and homogeneous mixture. The solution was added to 24-well plates and kept at 4 °C for 12 h. Next, the mold was placed at −20 °C and allowed to solidify for 24 h, followed by lyophilization of the chitosan scaffolds in a freeze dryer (Thermo, USA) for 24 h at −56 °C. The resulting scaffolds were removed and immersed in 0.1 M NaOH to neutralize the residual acetic acid. They were washed three times in 0.01 M PBS, 0.9 % NaCl and 75 % ethanol, respectively. Next, they were air-dried and stored until further use (Shi et al. 2012).

Determination of scaffold swelling ratio

Dry scaffolds were weighed on a precision balance (dry weight: W_d) and immersed in PBS for various lengths of time. After removal of the excess liquid from the surface by using a filter paper, the scaffolds were weighed again (swollen weight: W_s). The swelling ratio was calculated by using the following equation: swelling ratio (%) = $(W_s − W_d) / W_d \times 100$. This test was performed repeatedly and independently on seven different samples.

Scanning electron microscopy

Scanning electron microscopy was used to analyze the surface of the chitosan scaffolds containing attached DPSCs. The scaffolds were rinsed in PBS (pH 7.4) and fixed in a solution of 2 % glutaraldehyde and 0.6 % paraformaldehyde at 4 °C for 24 h. Next, they were dehydrated by being passed through a gradient series of acetone, dried in a critical point dryer and coated with gold-palladium. Samples were analyzed by using a scanning electron microscope (Hitachi S-2700, Tokyo, Japan) operated at an accelerating voltage of 20 kV. The test was repeated on seven different samples (Gaspar et al. 2011).

Viability of co-cultured cells

The chitosan scaffolds co-cultured with DPSCs for 24 h, 48 h, or 72 h were carefully removed from the 6-well plates and washed twice with PBS. The chitosan scaffolds with attached cells were digested by using 0.25 % trypsin and the cells were collected by centrifugation at 1000 rpm for 5 min. In subsequent assays, cells detached from the chitosan scaffolds are referred to as chitosan cells, whereas fresh DPSCs not co-cultured with chitosan scaffolds are referred to as negative cells. Both chitosan cells and fresh DPSCs were cultured further in 96-well plates at a density of 6000 cells per well, in 100 μl DMEM/F12 medium supplemented with 10 % fetal bovine serum (FBS). They were incubated at 37 °C under 5 % CO_2 and 95 % air in a humidified incubator. Cell viability was measured by using the Cell Counting Kit-8 (CCK-8) assay (Beyotime, China) in conditioned media harvested from the following wells: the chitosan group (media incubated with chitosan cells), the positive control (media containing 0.01 g/l lead acetate), the normal group/negative control (media incubated with fresh DPSCs) and the control group (media without any cells). Before measuring the absorbance (A), 10 μl CCK-8 was added to each well and incubated for 1 h at 37 °C. The optical density was then measured at 450 nm by using a multi-mode microplate reader (BioTek, Synergy2, USA). Cell viability was calculated by using the equation: Cell Viability (%) = $(A_{experiment} − A_{control})/A_{normal} \times 100$

b-NGF/BDNF/GDNF/NT-3 enzyme-linked immunosorbent assay

To quantify the neurotrophins produced by DPSCs, conditioned medium was taken from cells at passages two to four, cultured for 48 h and analyzed by enzyme-linked immunosorbent assay (ELISA) with E_{MAX}Immuno-assay kits (Promega, Southampton, UK) for human b-nerve growth factor (b-NGF),

brain-derived neurotrophic factor (BDNF), glial-cell-derived neurotrophic factor (GDNF) and neurotrophin-3 (NT-3), according to the manufacturer's instructions. Briefly, a standard curve was constructed by using the provided neurotrophins standards and test samples of conditioned medium at various dilutions were run in duplicate after acid treatment, with neurotrophins concentrations being extrapolated from the standard curve.

Neural differentiation of DPSCs

To induce neural differentiation of DPSCs, cells were co-cultured with the chitosan scaffolds and cultured in growth medium supplemented with neural induction medium containing 2 % B27, 2 % N2 (PAA Laboratories, Coelbe, Germany), 25 ng/ml BDNF, 40 ng/ml NGF and 25 ng/ml bFGF (R&D Systems, Minneapolis, Minn, USA). After 14 days in vitro, reverse transcription plus the polymerase chain reaction (RT-PCR), Western blotting and immunofluorescence assays were employed to detect the neural differentiation of DPSCs (see below; Xu et al. 2013).

RT-PCR analysis

Total cellular RNA was isolated from cells and reverse-transcribed by using conventional protocols. PCR amplification was performed with the following primer sets: D-glyceraldehyde-3-phosphate dehydrogenase (GAPDH) 5′-TCCATGACAACTTTGGTATCG-3′, 5′-TGTAGCCAAATTCGTTGTCA-3′; 2′,3′-cyclic-nucleotide 3′-phosphodiesterase (CNPase) 5′-CACCATGCACCTCTCCCAGC-3′, 5′-ATGGAGCCGATCCGGTCCAG-3′; glial fibrillary acidic protein (GFAP) 5′-GCTTCCTGGAACAGCAAAAC-3′, 5′-GGCTTCATCTGCTTCCTGTC; Nestin 5′-CTCTGACCTGTCAGAAGAAT−3′, 5′-CCCACTTTCTTCCTCATCTG-3′; mitogen-activated protein-2 (MAP-2) 5′-CTGGGTCTACTGCCATCACTC-3′, 5′-CCCCTTTAGGCTGGTATTTGA-3′. All the primer sequences were determined by using established GenBank sequences. The primers were used to amplify the duplicate PCRs. Each sample was analyzed in triplicate and GAPDH was used as a control.

Western blot analysis

Cells were lysed in the buffer consisting of 50 mM TRIS, 150 mM NaCl, 2 % sodium dodecyl sulfate (SDS) and a protease inhibitor mixture. After centrifugation at 12,000 rpm for 12 min, protein concentrations were determined by using the Bradford assay (Bio-Rad). The resulting supernatant (50 μg protein) was subjected to SDS-polyacrylamide gel electrophoresis (PAGE). The separated proteins were transferred onto polyvinylidene difluoride membranes at 350 mA for 2.5 h in a blotting apparatus (Bio-RAD, Calif., USA). Membranes were blocked with 5 % nonfat milk and incubated with primary antibodies (1:400) at 4 °C overnight and subsequently with anti-rabbit or anti-mouse horseradish-peroxidase-conjugated secondary antibodies (1:1000) for 2 h at room temperature. Concomitantly, GAPDH was run as a reference protein. The following primary antibodies were used: GAPDH (anti-rabbit, Santa Cruz), anti-nestin (anti-mouse, Sigma), anti-CNPase (anti-rabbit, Sigma), anti-GFAP (anti-rabbit, Sigma), anti-MAP-2 (anti-rabbit, Sigma), anti-β-catenin (anti-rabbit, Sigma), anti-GSK3-β (anti-rabbit, Sigma) and anti-active-caspase3 (anti-rabbit, Sigma).

Immunofluorescence analysis

At 14 days after co-culture of DPSCs with the chitosan scaffold, the scaffold was fixed in 4 % paraformaldehyde in 0.1 M PBS for 1 h and washed with ice-cold PBS. After being embedded in O.C.T. (SAKURA, USA), the scaffolds were sectioned into 15-μm-thick sections by using a cryostat (Leica CM1950, Germany) and the sections were mounted on poly-lysine-coated glass slides. After being dried at room temperature for 30 min, the sections were blocked and then incubated with mouse monoclonal anti-β-catenin, anti-CNPase, anti-GFAP and anti-MAP-2 for 2 h at room temperature. The sections were subsequently washed with PBS, incubated with Alexa-Fluor-568-conjugated anti-mouse IgG for 2 h at room temperature and finally counterstained with 4,6-diamidino-2-phenylindole (DAPI; 1:1000, Sigma) for 15 min at 4 °C. The cells were examined by using a Leica fluorescence microscope (Germany).

Spinal cord injury

Experiments were performed in accordance with the National Institutes of Health Guidelines for the Care and Use of Laboratory Animals; all animal protocols were approved by the Department of Animal Center, Medical College of Nantong University. Male Sprague–Dawley rats ($n = 70$) with an average body weight of 250 g (220–275 g) were used. Rats were anesthetized with sodium pentobarbital (50 mg/kg, i.p.), the thoracic back area was shaved and disinfected with povidone iodine and a laminectomy was then performed at the T9 spinal cord level with the dura mater intact. Contused incomplete SCI was induced by dropping a 10-g weight rod from a 75-mm height onto the exposed dorsal surface of the spinal cord by using an NYU impactor (Cho et al. 2009). During the recovery period, body temperature was maintained at 37 °C in a heated chamber. Postoperative care included bladder expression 1–2 times per day until bladder function had recovered. Prophylactic kanamycin (1 mg/kg) was regularly administered for 1 week after surgery.

Cell transplantation, locomotor function and hematoxylin and eosin staining

One week after SCI, the injured rats were randomly assigned to four groups without bias: DPSC-treated ($n = 17$), the DPSC/chitosan-scaffold-treated ($n = 18$), PBS-treated ($n = 18$) and control ($n = 17$) groups. Rats were fixed in a stereotaxic frame (Stoelting, Wood Dale, Ill., USA). A 25-gauge cannula connecting to a 10-μl Hamilton syringe was used to transplant a total of 10 μl cultured cells (2.5×10^5 cells) into the epicenter of the injury over a 10-min period (infusion rate: 60 μl/h) after reopening the wound. All rats received cyclosporine A (10 mg/kg, i.p.) daily from 2 days before the transplantation until the completion of this experiment in order to suppress an immune rejection. The spontaneous recovery of locomotor function after SCI was examined by using the Basso, Beattie and Bresnahan (BBB) rating scale (Basso et al. 1995). For hematoxylin and eosin (H&E) staining, spinal cord samples were fixed in 10 % formal solution, embedded in paraffin and sliced into cross-sections of 7-μm thickness at two spinal cord levels (2 mm rostral and caudal to the epicenter of injury). These sections were then stained with H&E.

Double-staining of TUNEL and DAPI

To detect cell apoptosis in the spinal cord, double-staining of DAPI and terminal deoxynucleotidyl transferase-mediated dUTP nick end labeling (TUNEL) was performed on transverse sections after transplantation. Following immunohistochemical staining of DAPI, as described above, TUNEL was performed by using the In Situ Cell Death Detection Kit (Roche Diagnostics).

Statistical analysis

All data are shown as means ± SEM from at least three independent experiments, each being performed with triplicate samples. Differences between groups were tested for statistical significance by means of analysis of variance. Student's *t*-test was used to determine significance with SPSS 16.0 software. Values for $P < 0.05$ were considered as being statistically significant.

Results

Characterization of chitosan scaffolds and secretion of neurotrophic factors by cultured DPSCs

We designed the shape of the chitosan scaffolds based on the shape of a flat-bottomed 24-well plate. Chitosan scaffolds of approximately 16 mm in diameter and 5 mm in thickness were produced (Fig. 1a, b). Their swelling ratio was 86.53

± 12.46 % in PBS at 37 °C indicating that the chitosan scaffolds were extremely hydrophilic, with the capacity to accommodate large quantities of saline solution within their three-dimensional structure. Scanning electron microscopy revealed the morphology and surface structure of the porous chitosan scaffolds and of the DPSCs that had migrated within the microporous structure. The pores were interconnected and the pore size was 268.79 ± 13.25 μm on average (Fig. 1c, d). The cytotoxic profile of DPSCs on the chitosan scaffolds was measured via MTT assay. The results showed that the viability of DPSCs was not influenced by co-culture with the chitosan scaffolds compared with the normal group (conditioned media harvested from fresh DPSCs). However, as expected, the lead acetate treatment markedly decreased cell viability. These results indicated that DPSCs grew well within the chitosan scaffolds and that the chitosan scaffolds possessed no obvious cytotoxicity (Fig. 1e). The concentrations of BDNF, GDNF, b-NGF and NT-3 secreted into the conditioned medium of the cultured DPSCs were determined by using ELISA. Compared with the control group, the levels of BDNF, GDNF, b-NGF and NT-3 were significantly increased in the DPSC/chitosan-scaffold group by 2.17-fold, 1.53-fold, 4.14-fold and 2.28-fold, respectively (Fig. 1f-i).
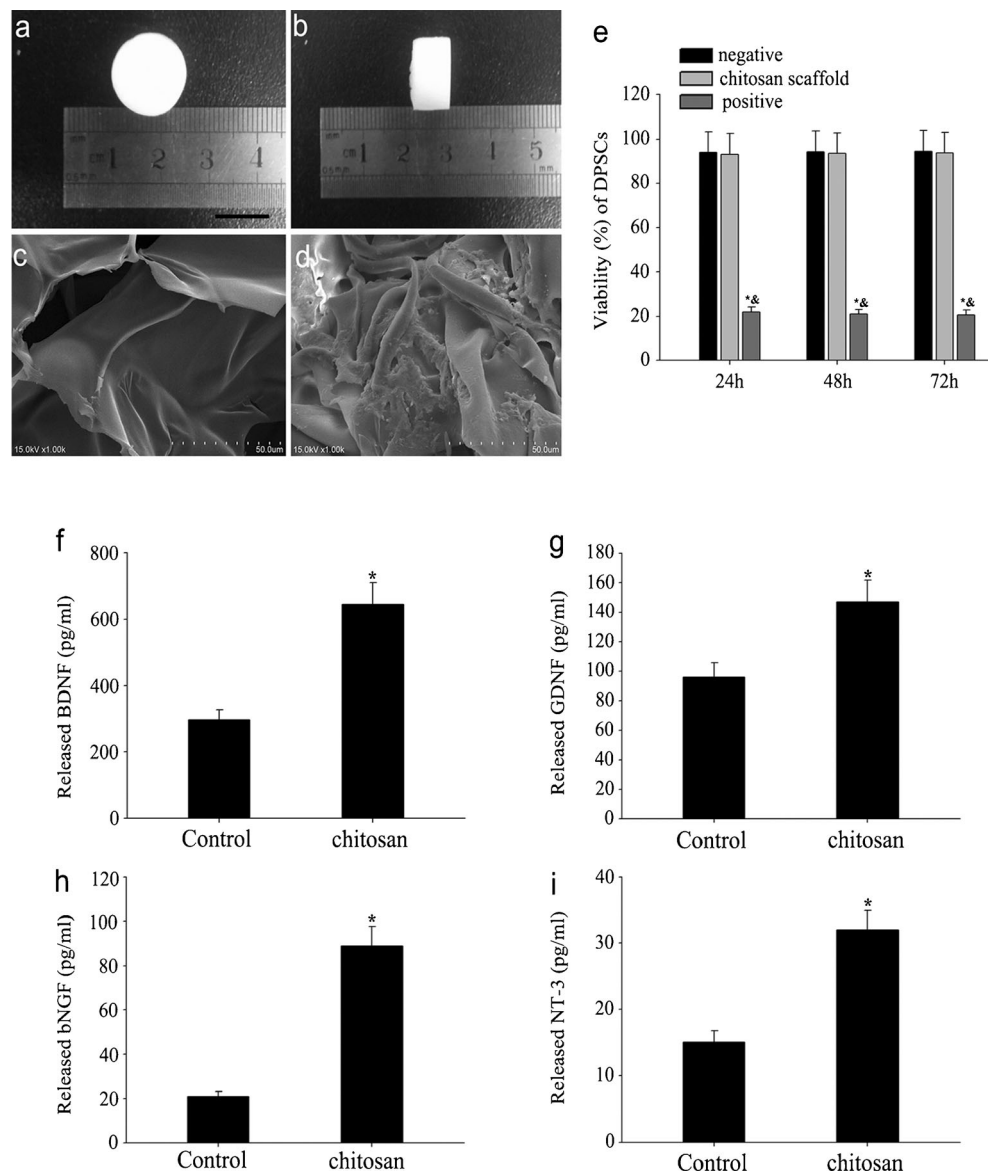
Effect of chitosan scaffolds on neural differentiation of DPSCs

To determine the effect of the chitosan scaffolds on the neural differentiation of DPSCs, the cells were grown in a differentiation medium without the chitosan scaffolds (the control group) or within the chitosan scaffolds and the expression of neuronal, astrocytic and oligodendrocytic markers was examined. After 14 days of induction with neural induction medium, DPSCs expressed neural-cell-specific markers CNPase (oligodendrocytes), GFAP (astrocytes) and MAP-2 (neurons). The levels of CNPase, MAP-2 and GFAP were higher in the DPSC/chitosan-scaffold group. Compared with the control group, the pan-neural progenitor marker nestin was expressed at low levels in the DPSC/chitosan-scaffold group (Fig. 2a, b). RT-PCR analysis demonstrated that, compared with the control group, a significantly declined expression of nestin and an upregulated expression of CNPase, GFAP and MAP-2 occurred in the DPSC/chitosan-scaffold group (Fig. 2c, d).

Chitosan-scaffold-induced neural differentiation of DPSCs was mediated by activation of Wnt/β-catenin signaling

In order to understand the underlying mechanisms for the DPSC→neural differentiation in response to chitosan scaffolds, we wished to examine the expression levels of β-catenin, phosphorylated β-catenin (p-β-catenin), GSK-3β and c-

Fig. 1 Characterization of chitosan scaffolds and secretion of neurotrophic factors by cultured dental pulp stem cells (DPSCs). **a, b** Shape of chitosan scaffolds as based on the shape of a well of a flat-bottomed 24-well plate (16 mm diameter, 5 mm thick). **c, d** Scanning electron microscopic images showing the morphology and surface structure of chitosan scaffolds and adhering DPSCs. The surface of the chitosan scaffolds was smooth with complex three-dimensional structures. ×1500. **e** Viability of DPSCs was not influenced by co-culture with the chitosan scaffolds. However, as expected, lead acetate treatment markedly decreased cell viability. **f–i** Neurotrophic factors concentration in DPSC culture medium were quantified by enzyme-linked immunosorbent assay (ELISA). ELISA indicated a significant increase in brain-derive neurotrophic factor (*BDNF*), glial-cell-derived neurotrophic factor (*GDNF*), neurotrophin-3 (*NT-3*) and b-nerve growth factor (*b-NGF*) levels after DPSC culture on chitosan scaffolds. *,&Statistically different from controls

myc. The results showed that, during the process of DPSC→ neural differentiation, the chitosan scaffolds significantly increased the expression of total β-catenin and decreased the expression of p-β-catenin. The total β-catenin protein expression level was significantly decreased and the p-β-catenin protein expression level was considerably increased in the β-catenin short interfering RNA (siRNA)-transfected DPSC/chitosan-scaffold group compared with those in the DPSC/chitosan-scaffold group (Fig. 3a, b). To further examine the increased nuclear accumulation of β-catenin in DPSCs in the presence or absence of the chitosan scaffolds, we used Western blot analysis to evaluate changes in nuclear and cytoplasmic β-catenin expression. The expression of β-catenin in the nucleus was significantly higher in the DPSC/chitosan-scaffold group compared with the control group. The protein expression level of β-catenin in the

nucleus was significantly decreased in the β-catenin siRNA-transfected DPSC/chitosan-scaffold group compared with the DPSC/chitosan-scaffold group. However, no differences were seen in β-catenin in the cytoplasm in the DPSC/chitosan-scaffold group, the control group, or the β-catenin siRNA-transfected DPSC/chitosan-scaffold group (Fig. 3c, d).

However, the expression of a key enzyme in the negative regulation of Wnt/β-catenin signaling, namely the expression of GSK-3β, was remarkably lower in DPSCs within the chitosan scaffolds compared with that in the control group. To examine further the expression of the target gene of Wnt/β-catenin signaling, we detected the expression of c-myc by Western blot analysis. After incubation with the chitosan scaffolds, the expression of c-myc in DPSCs within the chitosan scaffolds was significantly higher than that in the control
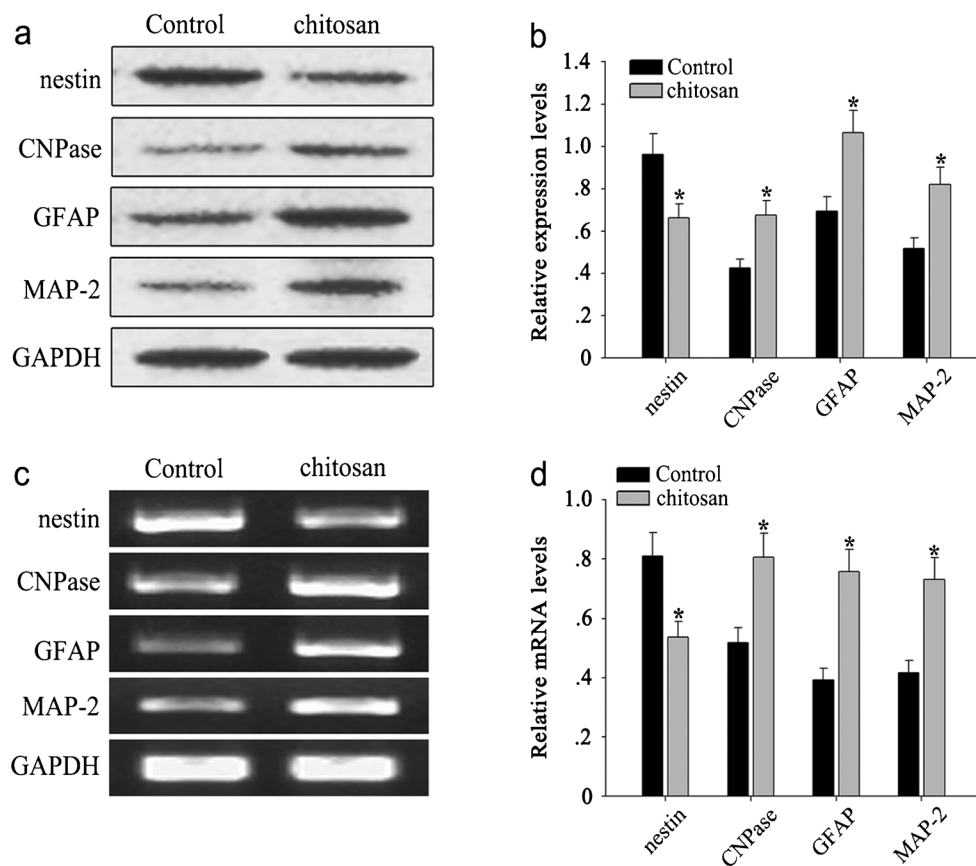
Fig. 2 Effect of chitosan scaffolds on neural differentiation of DPSCs. **a** Western blot analysis of nestin, 2′,3′-cyclic-nucleotide 3′-phosphodiesterase (*CNPase*), glial fibrillary acidic protein (*GFAP*) and mitogen-activated protein-2 (*MAP-2*) expression. CNPase, GFAP, and MAP-2 expression was significantly increased in the DPSC/chitosan-scaffold group compared with that in the control group. Compared with the control group, the pan-neural progenitor marker nestin was expressed at low levels in the DPSC/chitosan-scaffold group. D-glyceraldehyde-3- phosphate dehydrogenase (*GAPDH*) expression was determined as a control. **b** Quantification (relative optical density) of the intensity of staining of nestin, CNPase, GFAP and MAP-2 compared to GAPDH (*$P < 0.05$). **c** Total RNA was isolated after DPSCs were cultured with chitosan scaffolds, followed by reverse transcription plus the polymerase chain reaction (RT-PCR) analysis. **d** Quantitation of PCR products. Quantity of amplified product was analyzed by an image analyzer (*$P < 0.05$)

group. The β-catenin siRNA-transfected DPSCs within the chitosan scaffolds increased significantly their expression of GSK-3β and reduced their expression of c-myc (Fig. 3e, f).

Immunofluorescence staining showed GSK-3β was decreased in the chitosan scaffolds group, whereas GSK-3β was up-regulated in the β-catenin siRNA-transfected DPSC/chitosan-scaffold group. Immunofluorescence staining revealed the increased nuclear accumulation of β-catenin in DPSCs co-cultured with the chitosan scaffolds but this was inhibited by the β-catenin siRNA. The β-catenin siRNA had a negative effect on the chitosan-scaffold-induced higher c-myc expression level (Fig. 3g-o").

**Knockdown of β-catenin expression reversed effect of chitosan scaffolds on neural differentiation of DPSCs**

To assess the role of the Wnt/β-catenin signaling pathway on the chitosan-scaffold-induced neural differentiation of

DPSCs, we investigated whether β-catenin siRNA could elevate the neural differentiation potential in the chitosan-scaffold group. We found that the CNPase, MAP-2 and GFAP protein and mRNA expression levels were considerably decreased in the β-catenin siRNA-transfected DPSC/chitosan-scaffold group, compared with those in the chitosan-scaffold group (Fig. 4a-d). Immunofluorescence staining showed that the chitosan scaffolds had a positive effect on the expression of CNPase, MAP-2 and GFAP, with a significant inhibitory effect in the β-catenin siRNA-transfected DPSC/chitosan-scaffold group (Fig. 4e-m").

DPSCs ameliorated locomotor recovery after SCI

We investigated the potential therapeutic effect of DPSCs in SCI. Compared with rats treated with PBS and DPSCs, DPSC/chitosan-scaffold-treated rats showed a significant survival rate (Fig. 5a). Behavioral performance was evaluated in
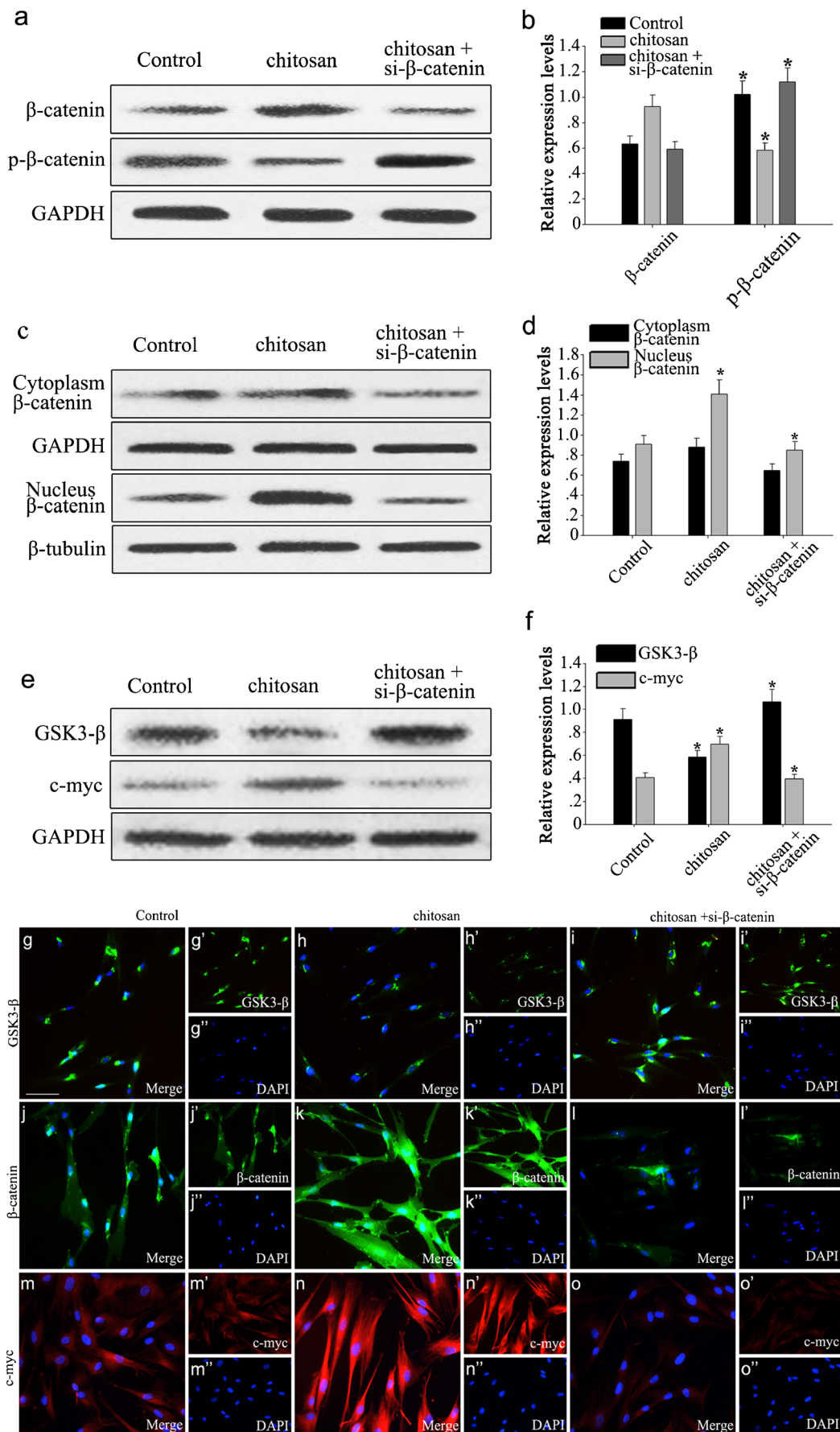
◀ **Fig. 3** Chitosan-scaffold-induced neural differentiation of DPSCs was mediated by activation of Wnt/β-catenin signaling. **a** Western blot analysis of β-catenin and phosphorylated β-catenin (p-β-catenin) protein expression (*chitosan* DPSC/chitosan-scaffold group, *chitosan + si-β-catenin* β-catenin siRNA-transfected DPSC/chitosan-scaffold group). **b** Quantification (relative optical density) of the intensity of staining of β-catenin and p-β-catenin relative to GAPDH (*$P < 0.05$). **c** Western blot analysis of β-catenin protein expression in cytoplasm and nucleus. **d** Quantification (relative optical density) of the intensity of staining of β-catenin relative to GAPDH (*$P < 0.05$). **e** Western blot analysis of GSK3-β and c-myc protein expression. **f** Quantification (relative optical density) of the intensity of staining of GSK3-β and c-myc relative to GAPDH (*$P < 0.05$). **g–o"** Immunofluorescence staining of GSK3-β (**g–i"**), β-catenin (**j–l"**) and c-myc (**m–o"**). Original magnification: ×200. *Bar* 50 μm

all rats that received DPSCs, DPSC/chitosan scaffolds, or PBS by using the BBB locomotor rating scale at weekly intervals for up to 60 days post-SCI. The results showed the locomotor function of the DPSC/chitosan-scaffold-treated rats significantly continued to increase to a final score of 14.28 ± 0.43, whereas the function of DPSC-treated rats was only 9.63 ± 0.64 at 60 days posttransplantation (Fig. 5b). To analyze histology and morphology after SCI, we performed H&E staining of the spinal cord in paraffin histopathological sections. The results revealed that the tissue loss, number of apoptotic cells and axon degradation in the DPSC/chitosan-scaffold-transplanted group were significantly lower than that in the other experimental groups, whereas no lesions were observed in the control group (Fig. 5c-c''', d–d''').

Detection of apoptosis in adult rat SCI after DPSC transplantation with chitosan scaffolds

To detect changes in cell apoptosis in spinal cord after DPSC transplantation with chitosan scaffolds, we first probed the expression of active-caspase3, an apoptosis maker, by Western blot (Fig. 6a, b). Active-caspase3 expression increased significantly in injured spinal cord, whereas it was almost undetectable in control groups. It decreased after DPSC transplantation. However, when DPSCs combined with chitosan scaffolds were transplanted after SCI, the expression of active-caspase3 was significantly reduced compared with that in injured rats and in rats with transplanted DPSCs alone. Furthermore, we performed double-staining of DAPI and TUNEL to detect the changes of cell apoptosis (Fig. 6c-j). On the injured side, the numbers of TUNEL-positive cells were observed to have increased more than that in the control groups in both the gray and white matter (Fig. 6c, g and d, h). However, TUNEL-positive cells decreased after DPSC transplantation. More interestingly, we noticed that the numbers of TUNEL-positive cells was strikingly reduced after DPSC/chitosan-scaffold transplantation compared with those in injured rats and in rats transplanted with DPSCs without chitosan scaffolds (Fig. 6c-j). These results suggested that

transplantation with DPSCs incubated on chitosan scaffolds significantly reduced cell apoptosis after SCI and that this was more efficient than that following DPSC transplantation alone.

Discussion

DPSCs have previously been investigated as a possible cell source for human regenerative therapies. However, this is the first time, to our knowledge, that the potential effect of the Wnt/β-catenin signaling pathway on neural differentiation of DPSCs combined with chitosan scaffolds has been explored. DPSCs have a higher neural differentiation capacity after combination with chitosan scaffolds. Therefore, DPSCs are considered as a useful alternative cell source for future clinical applications and SCI therapy.

In a previous study by Pisciotta and colleagues, STRO-1⁺/c-Kit⁺/CD34⁻ DPSCs showed a much lower efficiency of commitment compared with STRO-1⁺/c-Kit⁺/CD34⁺ DPSCs, as demonstrated by β-III tubulin expression and by the shift to a neuronal-like shape (Pierdomenico et al. 2005). The STRO-1⁺/c-Kit⁺/CD34⁺ DPSCs also expressed further markers, such as MAP-2, Neu-N and synapsin, confirming their substantial commitment toward a neuronal lineage. Therefore, we chose STRO-1⁺, c-Kit⁺ and CD34⁺ DPSCs for this study.

The scanning electron microscopic results indicated that the chitosan scaffolds had a suitable porosity and pore size within which DPSCs could adhere and grow. We obtained an average pore diameter of 268.79 ± 13.25 μm and a high swelling efficiency of 86.53 ± 12.46 %. The pore size is compatible with cell migration, axonal growth and the elaboration of dendrites. Several studies have demonstrated that chitosan-based scaffolds exhibit no cytotoxicity toward various cell types and have good in vitro biocompatibility (Sun et al. 2007; Zhang et al. 2008). In accordance with these previous studies, our data revealed acceptable biocompatibility and a lack of cytotoxicity for our chitosan scaffolds. The data of the CCK-8 assay strongly support this conclusion, implying that chitosan scaffolds are especially attractive in tissue engineering for the delivery of human DPSCs to sites of injury. Dental pulp has been determined to provide neurotrophic support favoring neural differentiation in vitro and in vivo (Lillesaar et al. 2003). In this sense, GDNF, which is required for neural differentiation and dendritic arborization, is highly expressed in dental pulp cells. Other studies have demonstrated that dental pulp from both rats and humans produce GDNF, BDNF and NGF mRNAs in vitro, favoring the survival and phenotypic neural characteristics of neurons (Nosrat et al. 2004). Our results showed that, after incubation with chitosan scaffolds, the levels of BDNF, GDNF, b-NGF and NT-3 were significantly increased in the medium.
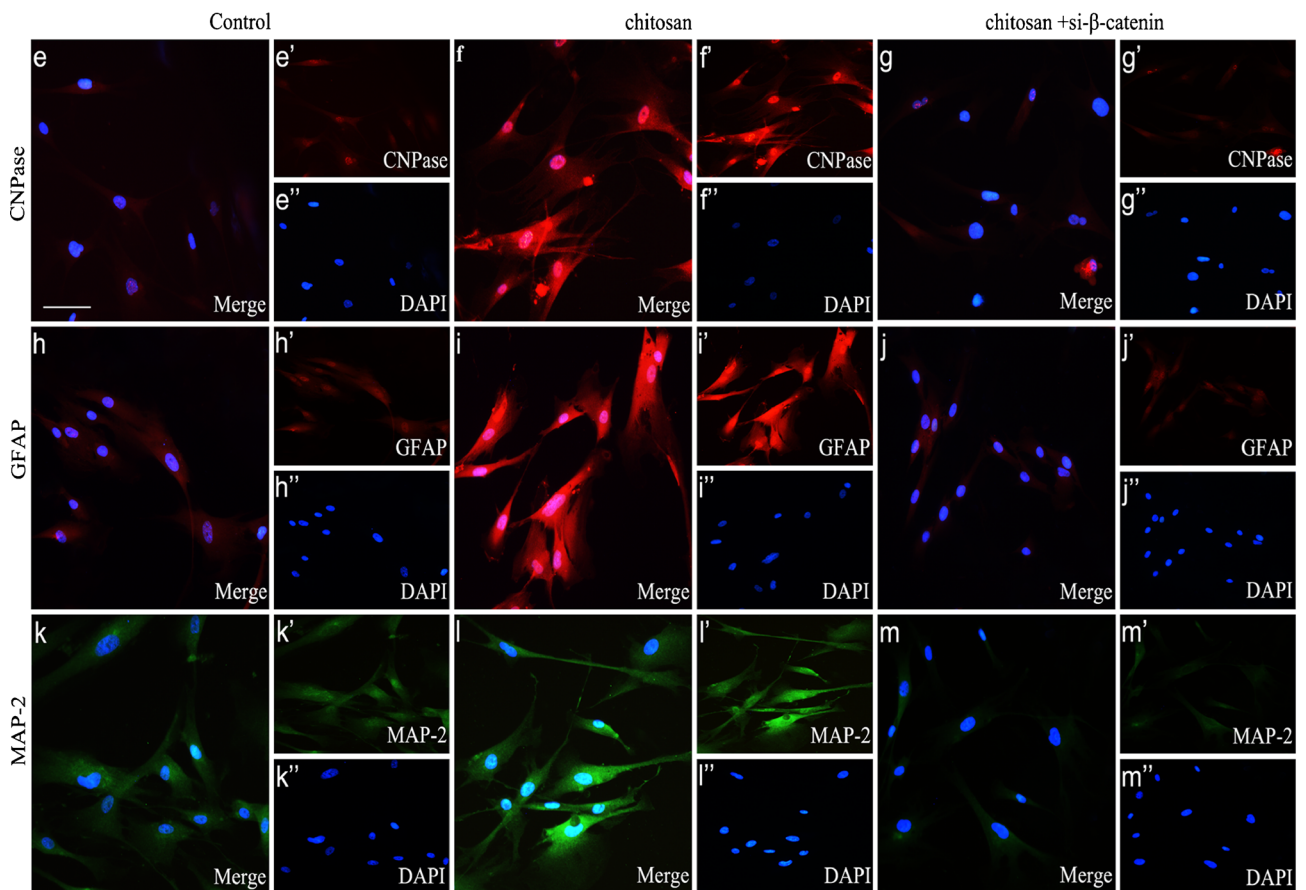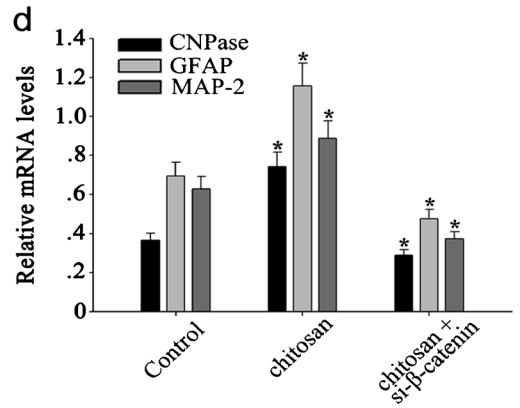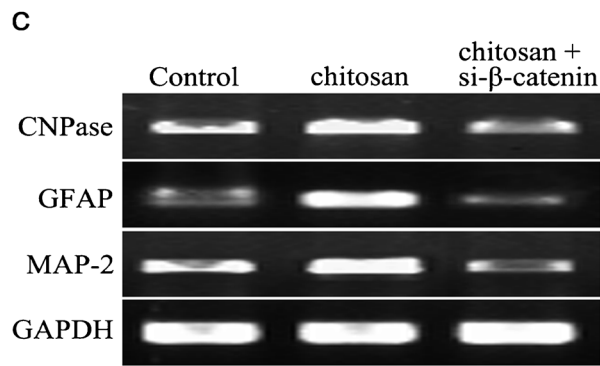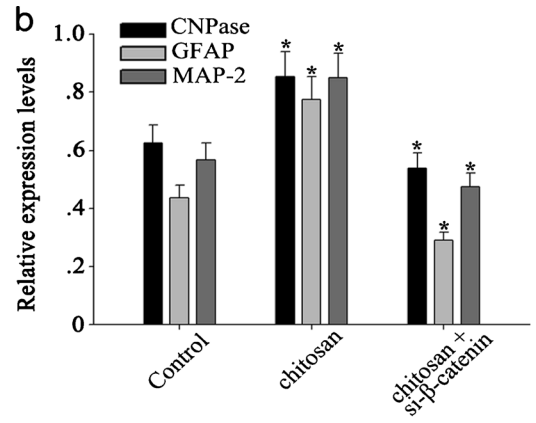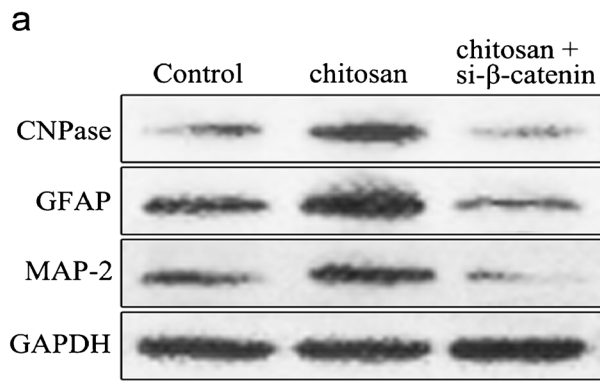
◀ **Fig. 4** Knockdown of β-catenin expression reversed the effect of chitosan scaffolds on neural differentiation of DPSCs. **a** Western blot analysis of CNPase, GFAP and MAP-2 protein expression. GAPDH expression was determined as a control. **b** Quantification (relative optical density) of the intensity of staining of CNPase, GFAP and MAP-2 relative to GAPDH (*$P < 0.05$). **c** RT-PCR analysis of CNPase, GFAP and MAP-2 mRNA expression. **d** Quantification (relative optical density) of the intensity of staining of CNPase, GFAP and MAP-2 relative to GAPDH (*$P < 0.05$). **e–m"** Immunofluorescence staining of CNPase (**e–g"**), GFAP (**h–j"**) and MAP-2 (**k–m"**). Original magnification: ×200. *Bar* 50 μm

Similar to BM-MSCs, DPSCs are able to differentiate into osteoblasts, chondrocytes and functionally active neurons in vitro, under defined conditions (Gronthos et al. 2000; Arthur et al. 2008). Cells, scaffolds and bioactive molecules are needed for neural tissue engineering, as for general tissue engineering. The differentiation and growth properties of dental pulp cells have recently been studied on a variety of natural scaffolds, including various types of chitosan, gelatin and collagen (Kim et al. 2009). The effect of a chitosan conduit on the proliferation and neural differentiation of human SHED under dynamic culture has also been examined (Su et al. 2013). In this study, we evaluated the potential of DPSCs on chitosan scaffolds to differentiate into multiple types of neural cells. The analysis of the differentiated cells by Western blot and RT-PCR established that DPSCs can indeed differentiate into GFAP+ astrocytes, MAP-2+ neurons and CNPase+ oligodendrocytes. Consistent with our previously published findings, we also identified higher levels of CNPase, MAP-2 and GFAP in the DPSC/chitosan-scaffold group compared with the control group (Feng et al. 2014b). Additionally, the pan-neural progenitor marker nestin is expressed at low levels in the DPSC/chitosan-scaffold group. These results indicate that DPSCs exhibit a
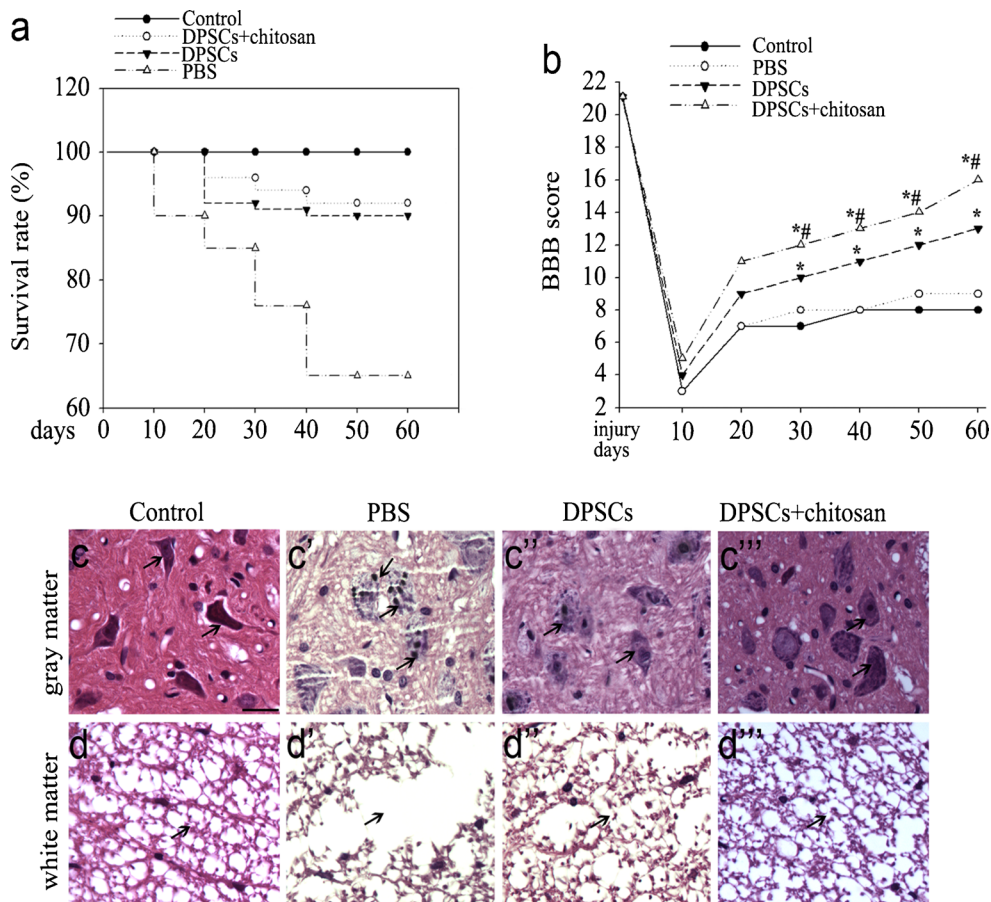
Fig. 5 DPSCs ameliorated locomotor recovery after SCI. **a** Survival curve. **b** Assessment of functional recovery by using the Basso, Beattie and Bresnahan (*BBB*) locomotor scale. Rats receiving transplants of DPSC/chitosan scaffold (*DPSCs+chitosan*) showed a statistically significant increase in hind limb function relative to that in the DPSC-treated groups (#$P < 0.05$) and the control groups (*$P < 0.05$), although scores improved in the DPSC-treated groups (*$P < 0.05$). **c-c'''**, **d–d'''** Histological and morphological assessment of SCI tissue at day 30 after injury in DPSC-treated, DPSC/chitosan-scaffold-treated, PBS-treated and control groups. No lesion was seen in the control group (**c**, **d**). The majority of typical characteristics of neuronal apoptosis including nuclear fragmentation, nuclear disappearance and nuclear pyknosis were found in the gray matter (**c'**, *black arrows*). Vacuoles, irregularly shaped spaces, axon degradation and disorders of organization were evident in the white matter (**d'**, *black arrows*). Tissue loss, number of apoptotic cells and axon degradation in the DPSC/chitosan-scaffold-transplanted group were significantly lower than that in the DPSC-treated group and the control group (**c''**, **c'''**, **d''**, **d'''**, *black arrows*). *Bar* 50 μm

Fig. 6 Expression of active-caspase3 and double-staining for DAPI and TUNEL in spinal cord after various interventions following SCI. **a** Spinal cord tissues from rats after various treatments after SCI were homogenized and subjected to immunoblot analysis. Sample immunoblots were probed for active-caspase3 and GAPDH. **b** Bar chart demonstrating the ratio of active-caspase3 to GAPDH at each time point. The data are means ± SEM ($n = 3$, $*P < 0.05$, significantly different from the sham groups). **c–j** Double-staining for DAPI and TUNEL on transverse sections of spinal cord obtained from transplantation and control groups. Changes of double-staining for DAPI and TUNEL in gray matter (**c–f**) and white matter (**g–j**) of spinal cord. Bar 20 μm (**c–f**), 50 μm (**g–j**). **k** Representation illustrating location of micrographs
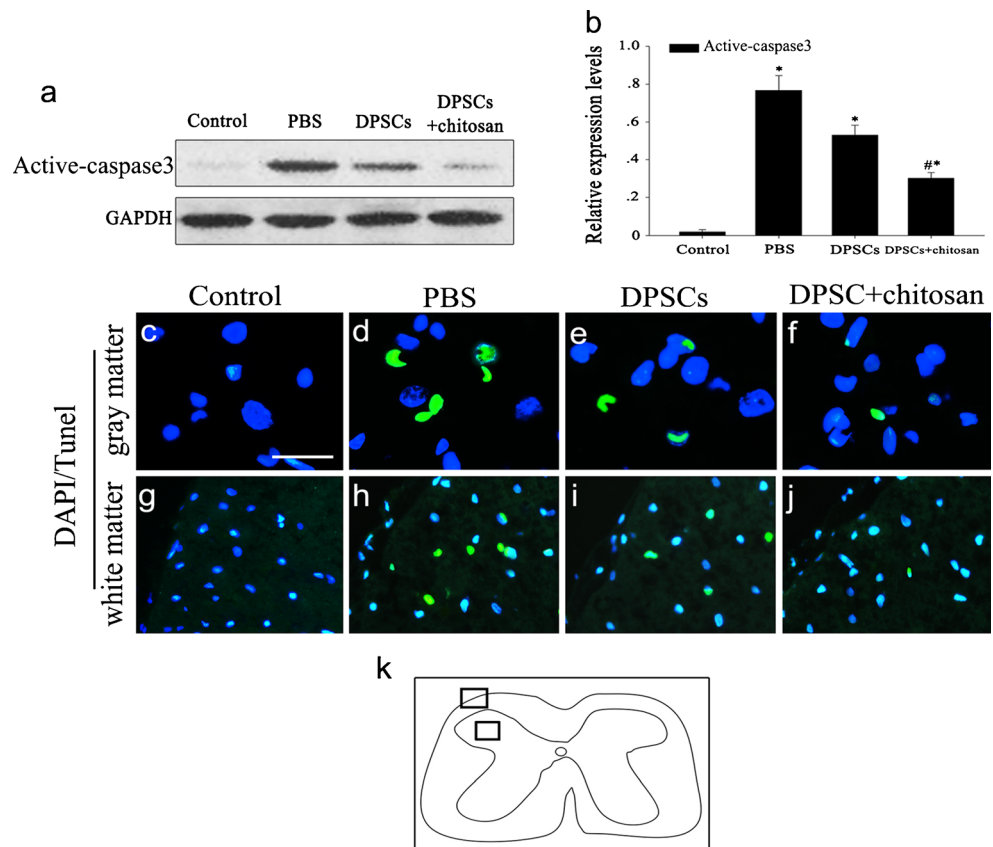
higher degree of neural differentiation potential in the chitosan scaffolds under neural differentiation culture.

The Wnt/β-catenin signaling pathway is essential for cell proliferation and cell fate determination (Espada et al. 2009). In recent years, several sets of data have suggested that the Wnt/β-catenin signaling pathway is elevated in the age-dependent neural differentiation of DPSCs. In our study, we have shown that total β-catenin expression and the nuclear accumulation of β-catenin increases in the DPSC/chitosan-scaffold group and that this accumulation can be inhibited by treatment with β-catenin siRNA. These results indicate that the chitosan-scaffold-induced neural differentiation of DPSCs is mediated by the activation of Wnt/β-catenin signaling. We examined the changes of neural differentiation in DPSCs after modulating Wnt/β-catenin signaling. After treatment with β-catenin siRNA, the CNPase, MAP-2 and GFAP protein and mRNA expression levels are considerably decreased. Taken together, these data allow us to conclude that Wnt/β-catenin signaling is an important mediator of neural differentiation in the DPSC/chitosan-scaffold group.

Functional recovery after SCI might be advanced with the use of cell-based therapy promoting strategic mechanisms including cellular replacement for neurons or glial cells after SCI and trophic or paracrine support for surviving or replaced cells in order to increase their survival and plasticity (Sharp and Keirstead 2007; Sakai et al. 2012). Before clinical trials,

sufficient preclinical data regarding the biological mechanisms of neurological improvement are required. Our results indicate that, compared with rats treated with PBS and DPSCs, DPSC/chitosan-scaffold-treated rats have a significantly better survival rate. Additionally, DPSCs combined with the chitosan scaffolds show earlier functional improvement as measured by the BBB locomotor rating scale. This can be explained on the basis that neurotrophic factors such as BDNF, GDNF, NT-3 and NGF or those secreted from transplanted stem cells enhance neural regeneration and improve neurological outcome, whereas the transdifferentiation of hematopoietic cells is reported to be extremely rare (Wagers et al. 2002; Lu et al. 2003; Koda et al. 2004). Our results also reveal that, after incubation with chitosan scaffolds, the levels of BDNF, GDNF, b-NGF and NT-3 are significantly increased in the medium. The tissue loss, number of apoptotic cells and axon degradation in the DPSC/chitosan-scaffold-transplanted group are significantly lower than those in the other experimental groups, whereas no lesions have been observed in the control group. Furthermore, the results of TUNEL-staining suggest that DPSC/chitosan-scaffold treatment can decrease cell apoptosis after SCI and more efficiently than DPSC transplantation only. Our findings strongly indicate that chitosan scaffolds can be used as a vector to support and transport DPSCs in order to initiate and facilitate nerve repair.

In summary, the development of chitosan scaffolds that can be combined with stem cells to provide a suitable vehicle for regenerative therapy is an important new field in biomaterial research. Additionally, the Wnt/β-catenin signaling pathway plays an important role during the neural differentiation of DPSCs that have been combined with chitosan scaffolds. The transplantation of DPSCs might therefore be a promising cell-based therapy for SCI, potentially extending the use of these cells to the treatment of other neurological diseases, especially if further therapeutic mechanisms are discovered.

References

Arthur A, Rychkov G, Shi S, Koblar SA, Gronthos S (2008) Adult human dental pulp stem cells differentiate toward functionally active neurons under appropriate environmental cues. Stem Cells 26:1787–1795

Basso DM, Beattie MS, Bresnahan JC (1995) A sensitive and reliable locomotor rating scale for open field testing in rats. J Neurotrauma 12:1–21

Bozkurt G, Mothe AJ, Zahir T, Kim H, Shoichet MS, Tator CH (2010) Chitosan channels containing spinal cord-derived stem/progenitor cells for repair of subacute spinal cord injury in the rat. Neurosurgery 67:1733–1744

Bray AF, Cevallos RR, Gazarian K, Lamas M (2014) Human dental pulp stem cells respond to cues from the rat retina and differentiate to express the retinal neuronal marker rhodopsin. Neuroscience 280:142–155

Ceruti S, Villa G, Genovese T, Mazzon E, Longhi R, Rosa P, Bramanti P, Cuzzocrea S, Abbracchio MP (2009) The P2Y-like receptor GPR17 as a sensor of damage and a new potential target in spinal cord injury. Brain 132:2206–2218

Cho SR, Kim YR, Kang HS, Yim SH, Park CI, Min YH, Lee BH, Shin JC, Lim JB (2009) Functional recovery after the transplantation of neurally differentiated mesenchymal stem cells derived from bone barrow in a rat model of spinal cord injury. Cell Transplant 18:1359–1368

Clevers H (2006) Wnt/beta-catenin signaling in development and disease. Cell 127:469–480

d'Aquino R, De Rosa A, Laino G, Caruso F, Guida L, Rullo R, Checchi V, Laino L, Tirino V, Papaccio G (2009) Human dental pulp stem cells: from biology to clinical applications. J Exp Zool B Mol Dev Evol 312B:408–415

Espada J, Calvo MB, Diaz-Prado S, Medina V (2009) Wnt signalling and cancer stem cells. Clin Transl Oncol 11:411–427

Feng X, Xing J, Feng G, Sang A, Shen B, Xu Y, Jiang J, Liu S, Tan W, Gu Z, Li L (2013) Age-dependent impaired neurogenic differentiation capacity of dental stem cell is associated with Wnt/beta-catenin signaling. Cell Mol Neurobiol 33:1023–1031

Feng X, Feng G, Xing J, Shen B, Tan W, Huang D, Lu X, Tao T, Zhang J, Li L, Gu Z (2014a) Repeated lipopolysaccharide stimulation promotes cellular senescence in human dental pulp stem cells (DPSCs). Cell Tissue Res 356:369–380

Feng X, Lu X, Huang D, Xing J, Feng G, Jin G, Yi X, Li L, Lu Y, Nie D, Chen X, Zhang L, Gu Z, Zhang X (2014b) 3D porous chitosan scaffolds suit survival and neural differentiation of dental pulp stem cells. Cell Mol Neurobiol 34:859–870

Gaspar VM, Sousa F, Queiroz JA, Correia IJ (2011) Formulation of chitosan-TPP-pDNA nanocapsules for gene therapy applications. Nanotechnology 22:015101

Giuliani A, Manescu A, Langer M, Rustichelli F, Desiderio V, Paino F, De Rosa A, Laino L, d'Aquino R, Tirino V, Papaccio G (2013) Three years after transplants in human mandibles, histological and in-line holotomography revealed that stem cells regenerated a compact rather than a spongy bone: biological and clinical implications. Stem Cells Transl Med 2:316–324

Gronthos S, Mankani M, Brahim J, Robey PG, Shi S (2000) Postnatal human dental pulp stem cells (DPSCs) in vitro and in vivo. Proc Natl Acad Sci U S A 97:13625–13630

Huang GT, Gronthos S, Shi S (2009) Mesenchymal stem cells derived from dental tissues vs. those from other sources: their biology and role in regenerative medicine. J Dent Res 88:792–806

Kas HS (1997) Chitosan: properties, preparations and application to microparticulate systems. J Microencapsul 14:689–711

Khor E, Lim LY (2003) Implantable applications of chitin and chitosan. Biomaterials 24:2339–2349

Kim H, Zahir T, Tator CH, Shoichet MS (2011) Effects of dibutyryl cyclic-AMP on survival and neuronal differentiation of neural stem/progenitor cells transplanted into spinal cord injured rats. PLoS One 6:e21744

Kim NR, Lee DH, Chung PH, Yang HC (2009) Distinct differentiation properties of human dental pulp cells on collagen, gelatin, and chitosan scaffolds. Oral Surg Oral Med Oral Pathol Oral Radiol Endod 108:e94–e100

Koda M, Hashimoto M, Murakami M, Yoshinaga K, Ikeda O, Yamazaki M, Koshizuka S, Kamada T, Moriya H, Shirasawa H, Sakao S, Ino H (2004) Adenovirus vector-mediated in vivo gene transfer of brain-derived neurotrophic factor (BDNF) promotes rubrospinal axonal regeneration and functional recovery after complete transection of the adult rat spinal cord. J Neurotrauma 21:329–337

Laino G, d'Aquino R, Graziano A, Lanza V, Carinci F, Naro F, Pirozzi G, Papaccio G (2005) A new population of human adult dental pulp stem cells: a useful source of living autologous fibrous bone tissue (LAB). J Bone Min Res 20:1394–1402

Lillesaar C, Arenas E, Hildebrand C, Fried K (2003) Responses of rat trigeminal neurones to dental pulp cells or fibroblasts overexpressing neurotrophic factors in vitro. Neuroscience 119:443–451

Lu P, Jones LL, Snyder EY, Tuszynski MH (2003) Neural stem cells constitutively secrete neurotrophic factors and promote extensive host axonal growth after spinal cord injury. Exp Neurol 181:115–129

Miura M, Gronthos S, Zhao M, Lu B, Fisher LW, Robey PG, Shi S (2003) SHED: stem cells from human exfoliated deciduous teeth. Proc Natl Acad Sci U S A 100:5807–5812

Nosrat IV, Smith CA, Mullally P, Olson L, Nosrat CA (2004) Dental pulp cells provide neurotrophic support for dopaminergic neurons and differentiate into neurons in vitro; implications for tissue engineering and repair in the nervous system. Eur J Neurosci 19:2388–2398

Pierdomenico L, Bonsi L, Calvitti M, Rondelli D, Arpinati M, Chirumbolo G, Becchetti E, Marchionni C, Alviano F, Fossati V, Staffolani N, Franchina M, Grossi A, Bagnara GP (2005) Multipotent mesenchymal stem cells with immunosuppressive activity can be easily isolated from dental pulp. Transplantation 80:836–842

Sakai K, Yamamoto A, Matsubara K, Nakamura S, Naruse M, Yamagata M, Sakamoto K, Tauchi R, Wakao N, Imagama S, Hibi H, Kadomatsu K, Ishiguro N, Ueda M (2012) Human dental pulp-derived stem cells promote locomotor recovery after complete transection of the rat spinal cord by multiple neuro-regenerative mechanisms. J Clin Invest 122:80–90

Sharp J, Keirstead HS (2007) Therapeutic applications of oligodendrocyte precursors derived from human embryonic stem cells. Curr Opin Biotechnol 18:434–440

Shi W, Nie D, Jin G, Chen W, Xia L, Wu X, Su X, Xu X, Ni L, Zhang X, Zhang X, Chen J (2012) BDNF blended chitosan scaffolds for

human umbilical cord MSC transplants in traumatic brain injury therapy. Biomaterials 33:3119–3126

Su WT, Shih YA, Ko CS (2013) Effect of chitosan conduit under a dynamic culture on the proliferation and neural differentiation of human exfoliated deciduous teeth stem cells. J Tissue Eng Regen Med (in press)

Sun G, Zhang XZ, Chu CC (2007) Formulation and characterization of chitosan-based hydrogel films having both temperature and pH sensitivity. J Mater Sci Mater Med 18:1563–1577

Wagers AJ, Sherwood RI, Christensen JL, Weissman IL (2002) Little evidence for developmental plasticity of adult hematopoietic stem cells. Science 297:2256–2259

Wei X, Zhang C, Gu Q (2010) Properties, products, and applications of chitosan. Chin J Reparative Reconstr Surg 24:1265–1270

Xu Y, Gu Z, Shen B, Xu G, Zhou T, Jiang J, Xing J, Liu S, Li M, Tan W, Feng G, Sang A, Li L (2013) Roles of Wnt/beta-catenin signaling in retinal neuron-like differentiation of bone marrow mesenchymal stem cells from nonobese diabetic mice. J Mol Neurosci 49:250–261

Yang Q, Du X, Fang Z, Xiong W, Li G, Liao H, Xiao J, Wang G, Li F (2014) Effect of calcitonin gene-related peptide on the neurogenesis of rat adipose-derived stem cells in vitro. PLoS One 9: e86334

Zhang J, Li D, Shen A, Mao H, Jin H, Huang W, Xu D, Fan J, Chen J, Yang L, Cui Z (2013) Expression of RBMX after spinal cord injury in rats. J Mol Neurosci 49:417–429

Zhang X, Yang D, Nie J (2008) Chitosan/polyethylene glycol diacrylate films as potential wound dressing material. Int J Biol Macromol 43: 456–462